Supplementary Data

A combinatorial approach for the discovery of cytochrome P450 2D6 inhibitors from nature

Johannes Hochleitner[1], Muhammad Akram[2], Martina Ueberall[1], Rohan A. Davis[3], Birgit Waltenberger[4], Hermann Stuppner[4], Sonja Sturm[4], Florian Ueberall[1+], Johanna M. Gostner[1]*, Daniela Schuster[2+]*

1 Division of Medical Biochemistry, Center for Chemistry and Biomedicine, Medical University of Innsbruck, Austria
2 Institute of Pharmacy / Pharmaceutical Chemistry, Computer Aided Molecular Design Group and Center for Molecular Biosciences Innsbruck (CMBI), University of Innsbruck, Austria
3 Griffith Institute for Drug Discovery, Griffith University, Brisbane, QLD 4111, Australia
4 Institute of Pharmacy / Pharmacognosy and Center for Molecular Biosciences Innsbruck (CMBI), University of Innsbruck, Austria
+ These authors contributed equally to this work
* Corresponding Author

Table of contents

In silico dataset for the screening of novel CYP2D6 inhibitors

Building of the 3D-database

Every single 2D-database was treated and built up separately using the BEST mode and creating a maximum of 255 conformers for each single substance in the 2D-database, according to the findings from the validation of the *in silico* workflow. From all of the 2,147 single substances that make up the 17 2D-databases we could recover 86 % *i.e.* 1,847 compounds that account for the 3D-databases, whereas 11 databases were built without declines and 6 databases were built with an overall loss of 300 compounds (Supplementary Table S1).

Screening of the 3D-database

We screened the 17 3D-databases with overall 1,847 compounds and applied a rigid search using the pharmacophore model for CYP2D6 inhibitors[1] that proved to be an appropriate tool in the preceding validation workflow. From the screened 1,847 compounds in 17 3D-databases, we identified 4.1 % *i.e.* 75 compounds that fitted the model for potential CYP2D6 inhibitors and that were located in 6 different 3D-databases. In 10 databases we were not able to identify compounds that fitted the pharmacophore model for CYP2D6 inhibitors (Supplementary Table S1).

Supplementary Table S1. *In silico* **dataset for the screening of novel CYP2D6 inhibitors.**

University Collaborators	Databases	Input 2D-database	Output 3D-database	Hits Total	Hits selected
Pharmacognosy_IBK	Birgit_C13_AR(+)_Birgit_MV26	2	2	-	-
Florianopolis_Brazil	Florianopolis_Falkenberg	3	3	-	-
Pharmacognosy_Graz	Polyacetylenes_from_Notopterygium	5	5	-	-
Pharmacognosy_IBK	Naturstoffe SKC-Files	7	7	-	-
Pharmacognosy_Vienna	lilo_krenn_compounds	13	13	-	-
Rohan_Davis	Rohan_Davis_Structures_II_checked	14	13	5	3
Pharmacognosy_IBK	Semisynthetika SKC-Files_CA_Isis	20	20	-	-
Pharmacognosy_Graz	Bupleurum_compounds	21	21	-	-
Pharmacognosy_Graz	Polyacetylenes_from_Oplopanax	29	29	-	-
Pharmacognosy_IBK	Semisynthetika CDX-Files	48	48	3	-
Pharmacognosy_IBK	Semisynthetika SKC-Files_AK_Isis	51	51	-	-
Pharmacognosy_IBK	Cdx-Files_Naturstoffe+Synthetika	56	56	3	-
Pharmacognosy_IBK	Naturstoffe CDX-Files	75	72	6	3
Pharmacognosy_Vienna	Atanasov_Vienna_NAT_library	114	109	-	-
Pharmacognosy_IBK	Substanzen_Pharmakognosie	236	221	9	-
Rohan_Davis	Rohan_Davis_NP_library_140704_cleaned	576	429	10	3
SPECS	Specs_NP_1mg_Jan2016_BEST_255	877	748	39	14
	Sum	**2,147**	**1,847**	**75**	**23**
	Recovery (%)	**100.0**	**86.0**	**4.1**	**1.2**

CYP2D6 inhibition of virtual hits already reported in the literature

In the course of the screening of the various databases we found 75 hits that fitted the pharmacophore model. From these hits, 23 were selected for the *in vitro* screening. We selected the hits according to non-available CYP2D6 inhibition data, plant origin and availability. The 52 not-tested hits included some duplicate entries and were composed of natural, synthetic or semisynthetic compounds. Focusing on the compounds from plant origin, highly potent and well-known CYP2D6 inhibitors were found by the pharmacophore model, like ajmalicine and quinidine. On the one hand, this was expected because some of these compounds have been used for model generation[1] already. On the other hand, additional active compounds were found, which underlines the power of the *in silico* pre-selection step (Supplementary Table S2).

Supplementary Table S2. Inhibitory potency of already tested inhibitors found by the model.

CAS	Name	Database	Inhibitory potency	Unit	IC_{50}/Ki	Classification	Reference
483-04-5	Ajmalicine	1	2.3	nM	IC_{50}	active	[2]
56-54-2	Quinidine	1	7.5	nM	IC_{50}	active	in-house
130-86-9	Protopine	1	78	nM	Ki	active	[3]
65-19-0	Yohimbine	1	0.062-0.72 (substrate dependent)	µM	IC_{50}	active	[4]
3520-14-7	Tetrahydro palmatine	1	3.04 ± 0.26	µM	IC_{50}	active	[5]
6018-39-9	Corypalmine	1	1-10	µM	IC_{50}	active	[6]
485-71-2	Cinchonidine	1	10	µM	IC_{50}	active	[7]
130-95-0	Quinine	1	10	µM	IC_{50}	active	[7]
2182-14-1	Vindoline	2	15.9	µM	IC_{50}	active	[2]
518-69-4	Corydaline	1	64.5 ± 9.8 (w/ preincubation)	µM	IC_{50}	weak	[8]
518-69-4	Corydaline	1	115.9 ± 7.6 (w/o preincubation)	µM	IC_{50}	inactive	[8]
10605-02-4	Palmatine chloride	1	92.6	µM	-	weak	[9,10]
115-53-7	Sinomenine	2	no inhibition at 50	µM	-	inactive	[11]
128-62-1	Noscapine	1	>100	µM	-	inactive	[12]
2688-77-9	Laudanosine	2	stated as inhibitor	-	-	unclear	[13]
482-74-6	Cryptopine	2	stated as inhibitor	-	-	unclear	[6]
databases: **1** Pharmacognosy Innsbruck, **2** SPECS							

Information on the compounds tested *in vitro*

Supplementary Table S3. All compounds tested *in vitro*. The numbers assigned are the same as in the manuscript.

Index	SciFinder CAS	Molecular weight incl. salts [g]	Name	Salt data
1	5629-60-7	368.43	Pteropodine	
2	5171-37-9	368.43	Isopteropodine	
3	29550-24-1	353.41	Thalictrivacine	
4	89647-69-8	531.48	Pistillarin	TFA
5	1620102-34-2	418.32	Secofascaplysic acid	TFA
6	61-25-6	375.85	Papaverine	HCl
7	2468-21-5	336.43	(+)-Catharanthine	
8	4837-77-8	526.42	Venenatine methiodide	CH3I
9	4781-58-2	487.56	(S)-Norreticuline	tosic acid
10	5001-20-7	336.45	(-)-Venalstonine	
11	3122-95-0	379.88	(+)-Laudanidine	HCl
12	477-30-5	371.42	Colcemid	
13	6871-44-9	420.94	Echitamine	HCl
14	175274-51-8	327.37	Spinosine	
15	73870-36-7	377.92	Des-N,O-dimethylarmepavine	HCl
16	559-48-8	380.44	(-)-Kopsine	
17	4939-81-5	322.42	(+)-Condylocarpine	
18	25651-04-1	327.37	Bracteoline	
19	485-19-8	429.81	(+)-Reticuline	HClO4
20	1936-18-1	327.37	(+)-Salutaridine	
21	476-32-4	353.37	(+)-Chelidonine	
22	4429-63-4	372.89	Tabersonine	HCl
23	4963-01-03	368.43	Isomitraphylline	
24	501-36-0	228.23	Resveratrol	
25	6591-63-5	782.94	2 Quinidine	H_2SO_4, 2 H_2O

Preparation of the compounds from the university collaborators-UIBK

The compounds **1** and **2** were isolated at the Institute of Pharmacy / Pharmacognosy, University of Innsbruck. The identification of the structure was performed by mass and NMR spectroscopy as well as by comparison (TLC, HPLC) with authentic samples. The compound **3** was isolated and identified as described previously[14].

Preparation of the compounds from the university collaborators-Rohan A. Davis

The isolation and identification of compounds **4** and **5** has been described elsewhere[15,16]. The compounds **6**, **7**, **21**, **22** and **23** were purchased from PhytoLab (www.phytolab.com).

Incubation conditions for the *in vitro* assay and the luminescence quenching control

Supplementary Table S4. Reaction volumes used of the CYP2D6 inhibition assay and the detection control of the P450-Glo reaction.

P450-Glo CYP2D6 inhibition assay (Promega)	[µl]
1 test compound	12.5
2 enzyme/substrate mix (CYP2D6/ME-luciferin-EGE)	12.5
3 NADPH regeneration system	25
4 detection reagent	50
total volume	100

inhibition control of the P450-Glo detection reaction	[µl]
1 test compound	12.5
2 enzyme/substrate mix (no CYP2D6/ luciferin-EGE)	12.5
3 NADPH regeneration system	25
4 detection reagent	50
total volume	100

Supplementary Table S5. Incubation conditions for the P450-Glo CYP2D6 inhibition pre-screen and for the P450-Glo detection reaction control

components	P450-Glo CYP2D6 inhibition pre-screen		P450-Glo detection reaction
	final concentrations for CYP2D6 reaction	addition of detection reagent	
test compound	100 µM	50 µM	50 µM
ME-luciferin-EGE	30 µM	~15 µM	- -
luciferin-EGE	- -	~0.75 µM	0.75 µM
KPO$_4$ buffer at pH 7.4 (K$_2$HPO$_4$/KH$_2$PO$_4$, 0.8/0.2)	100 mM	100 mM	100 mM
rhCYP2D6 baculosomes	0.25 pmol	0.125 pmol	- -
NADP+	1.30 µM	0.65 µM	0.65 µM
glucose-6-phosphate	3.30 µM	1.15 µM	1.15 µM
MgCl$_2$	3.30 µM	1.15 µM	1.15 µM
glucose-6-phosphate dehydrogenase	0.40 U/ml	0.20 U/ml	0.20 U/ml
sodium citrate pH 5.5	0.05 mM	0.025 mM	0.025 mM
DMSO concentration	1 %	0.5 %	0.5 %
detection reagent	-	50 µl	50 µl
total volume incl. detection reagent	-	100 µl	100 µl
reaction volume	50 µl	-	100 µl

Incubation times

	P45-Glo CYP2D6 inhibition pre-screen	P450-Glo detection reaction
pre-incubation	10 min	- -
CYP2D6 enzyme reaction	45 min	- -
stabilization of luminogenic signal	20 min	20 min

Plate reader settings

|	
signal detection integration time	1s
attenuation	automatic

Concentration-response curves of the strongest inhibitors
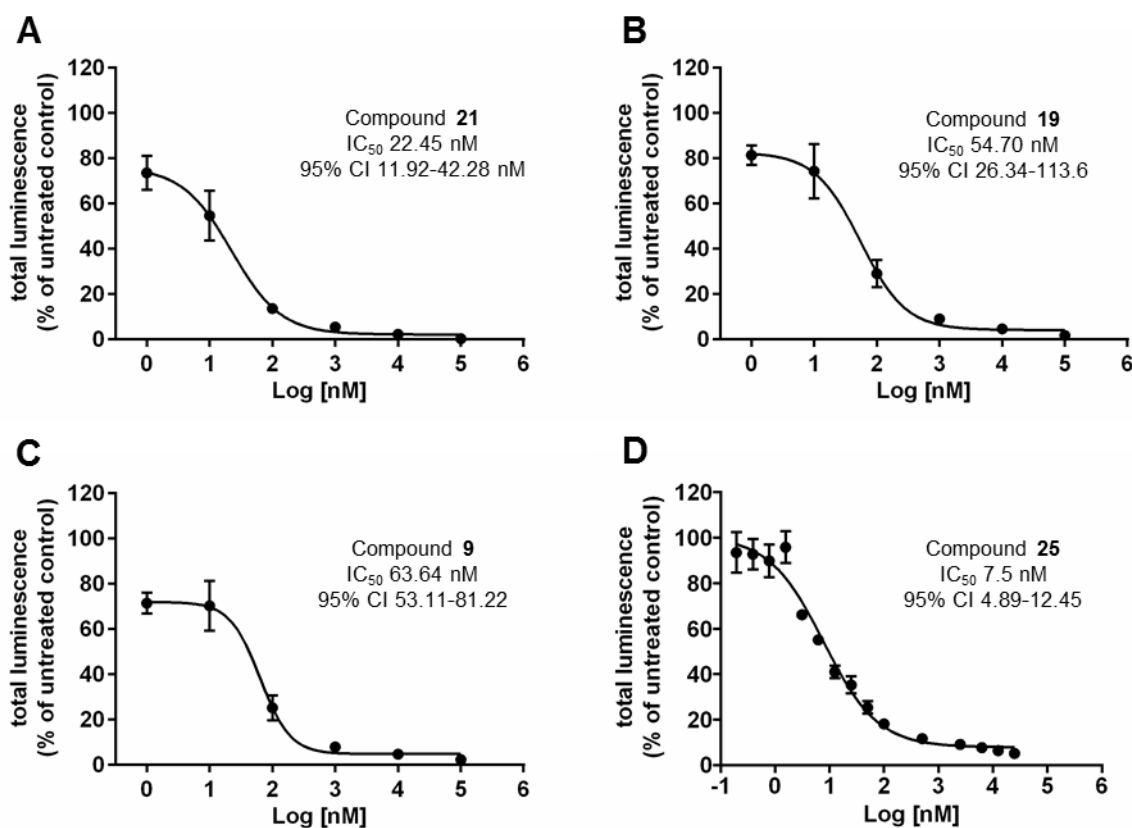
Supplementary Figure S1. Concentration-response curves for the three most potent inhibitors. IC$_{50}$ values were determined for the compounds, which showed a total luminescence greater than 50 % at 100 µM in the inhibition assay for P450-Glo CYP2D6. The compounds **21** (A), **19** (B) and **9** (C) turned out as strong inhibitors of CYP2D6 activity as their IC$_{50}$ values were in the lower nanomolar range. The IC$_{50}$ value for the model inhibitor **25** was comparable to the values reported in the literature (D). The error bars indicate the standard error of mean of triplicate measurements obtained in three independent experiments.

Establishment of the re-docking process

In order to predict the binding pose of an inhibitor in the active site cavity, the program settings were validated by re-docking of ligands to a CYP2D6 structure that was solved as a co-crystallized complex with inhibitors in the active site cavity by Wang et al (PDB entry 4WNT[19]). The re-docking helps to identify the software settings with which the crystallographic and thus known binding pose can be reproduced by a computational docking method within a range of a root mean square deviation (RMSD) at or below 2 Å. The re-docking experiments were performed using the genetic algorithm implemented in GOLD[17,18]. Independent re-docking models for each of the crystal structures 4WNT[19], 4WNU[19] and 4XRZ[20] were generated that exhibit a RMSD of 0.19, 0.95 and 0.60 Å for the core to the co-crystallized ligand compared to the re-docked ligand, respectively. Furthermore, each re-docking model was challenged with a self-generated ligand to avoid bias by using the bioactive conformation of the ligand for re-docking. For all three crystal structures *i.e.* 4WNT, 4WNU and 4XRZ, the RMSD of the core, co-crystallized ligand to the self-generated re-docked ligand was 0.37, 0.51 and 0.74, respectively. The docking and re-docking workflow obtained from 4WNT, with ajmalicine co-crystallized in the active site cavity (Supplementary Fig. S2) turned out to be best suited for the further studies.
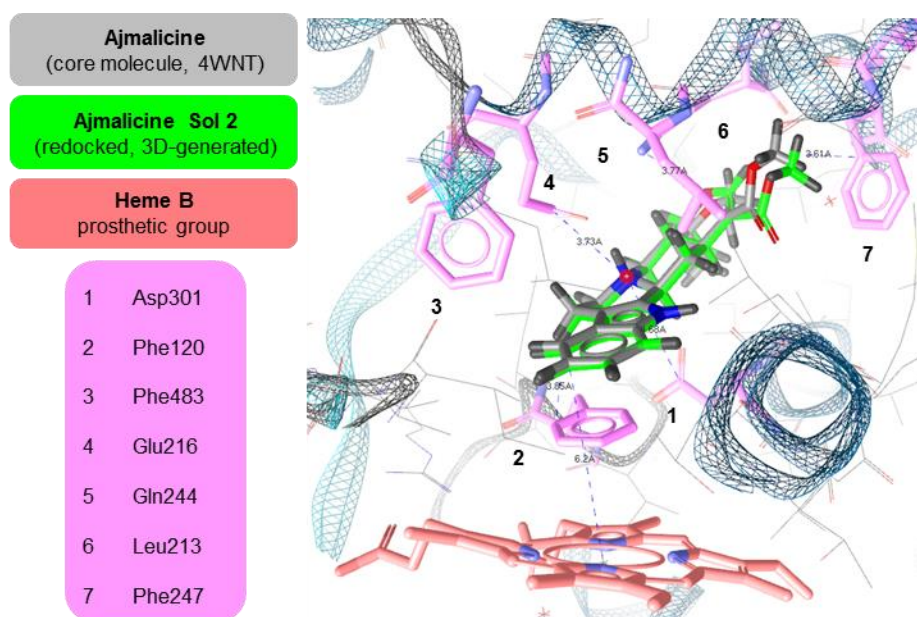
Supplementary Figure S2. Visualization of ajmalicine in the active site cavity of CYP2D6 with a docking model. The docking model for CYP2D6 was based on the crystal structure co-crystallized with the inhibitor ajmalicine (PDB code 4WNT), having a RMSD value below 0.4 Å of the core molecule to the re-docked molecule. The amino acids highlighted in magenta listed on the left side were found to be important interaction and binding partners in previous studies. The prosthetic heme-b group is highlighted in red.

# Interactions of the three most potent inhibitors in the active site cavity of 4WNT

Supplementary Table S6. The three most potent inhibitors that were docked in the active site cavity of 4WNT showed the following interactions with the macromolecule:

Chelidonine			
ligand	enzyme-AA	mode of interaction	distance Å
Benzene ring	Phe120	Van der Waals	3.1
Protonated N	Glu216	ionic	3.6
	Gln244	electrostatic	3.8
	Ser304	H-bond	4.4
Phenantridin-6-ol	Glu216	H-bond	2.8
Dioxolo	Asp301	H-bond	4.5
Reticuline			
ligand	enzyme-AA	mode of interaction	distance Å
Benzene ring (isoquinoline)	Phe120	Van der Waals	3.6
Protonated N	Glu216	ionic	3.1
Hydroxyphenyl-OH	Asp301	H-bond	2.3
Isoquinoline-7-OH	Ser304	H-bond	4.7
(S)-Norreticuline			
ligand	enzyme-AA	mode of interaction	distance Å
Benzene ring	Phe120	Van der Waals	3.8
Protonated N	Glu216	ionic	5.1
	Asp301	ionic	3.3
Isoquinoline-7-OH	Gln244	H-bond	3.6
	Ser304	H-bond	4.6

Comparison of the docking poses in different PDB structures

Supplementary Figure S3. Comparison of the docking poses of the three most potent inhibitors in different PDB structures: The docking model selected in the redocking process was used for the prediction of the potential binding poses of the newly found inhibitors. Figure S3 shows the compounds **21** (I), **19** (II) and **9** (III), which were the three most potent inhibitors in the *in vitro* screening. Each compound was docked in the active site cavity of the PDB structures 4WNT[19], 4WNU[19] and 4XRZ[20], respectively. For a better comparison, the docked inhibitor is presented on the left sides, whereas the core and the redocked core molecule of the corresponding crystal structure can be found on the right sides (I, II and III_A-F). The docked inhibitors are colored in grey/light blue, the heme-moiety in yellow and the amino acids in magenta. The numbers indicate the follwing amino acids: 1-Ser304, 2-Asp301, 3-Phe120, 4-Phe247, 5-Glu216, 6-Leu213, 7-Gln244 and 8-Phe483.

II_A II_B II_C II_D II_E II_F
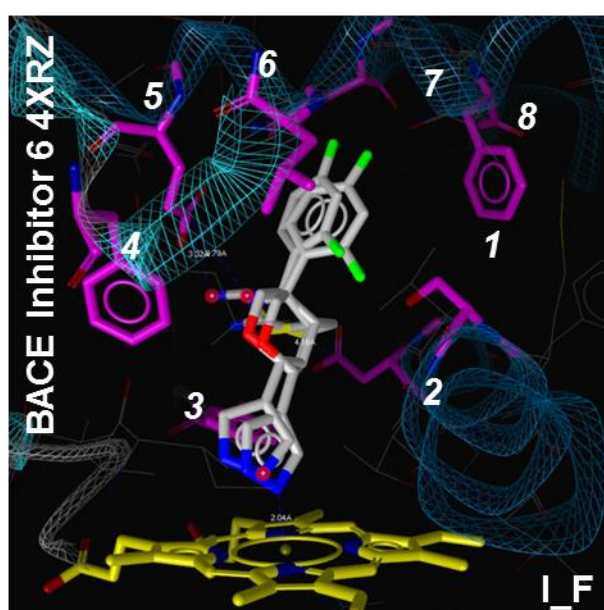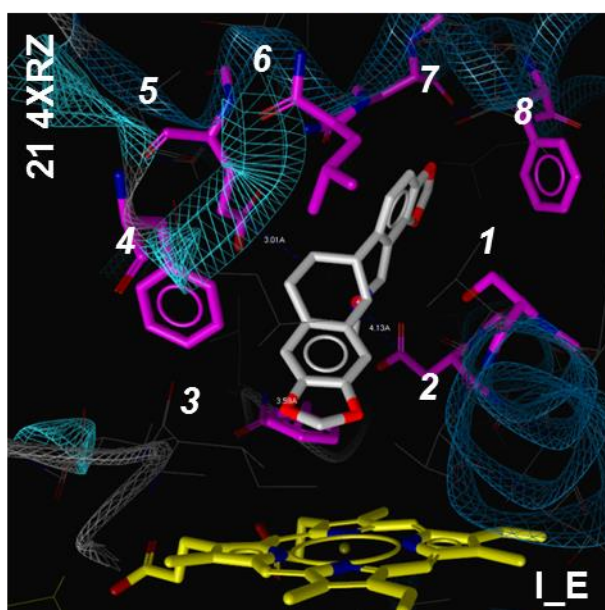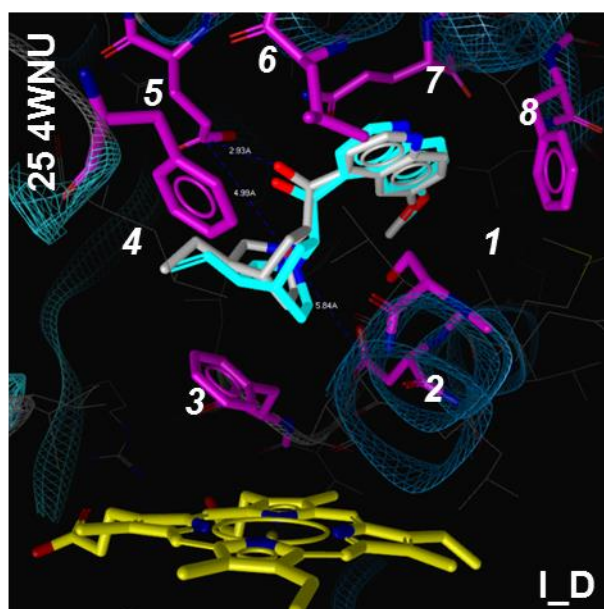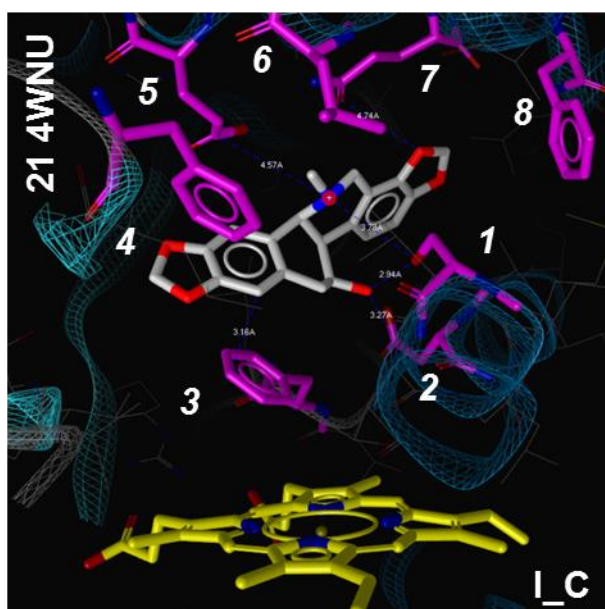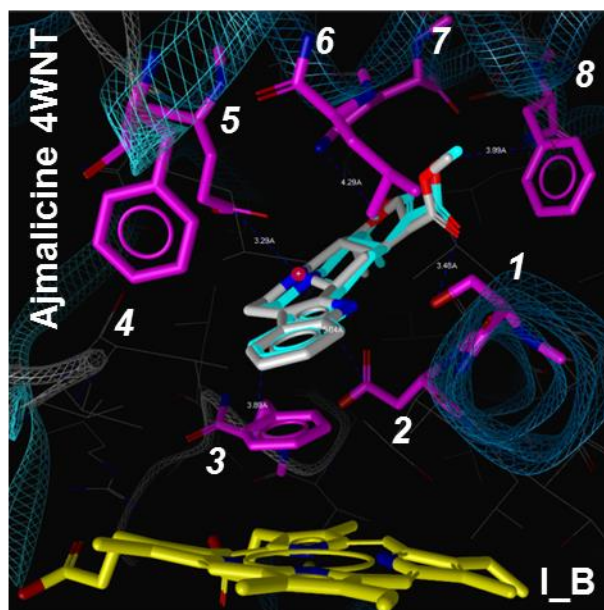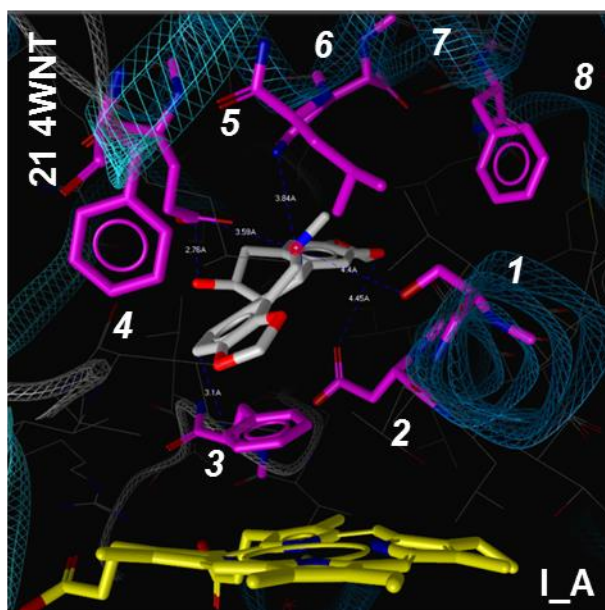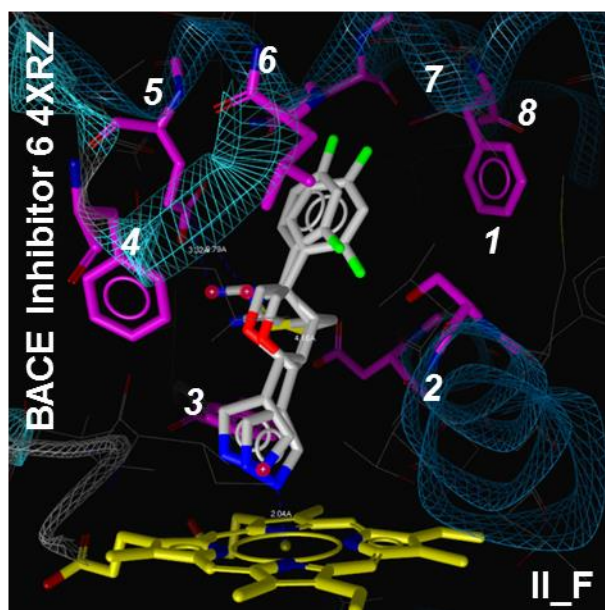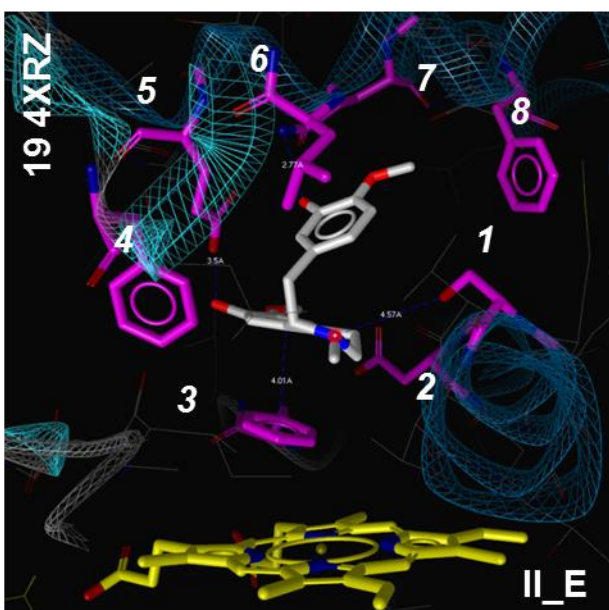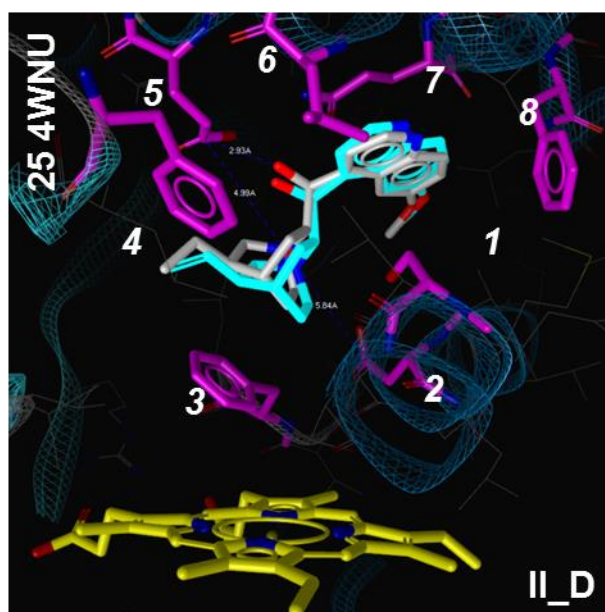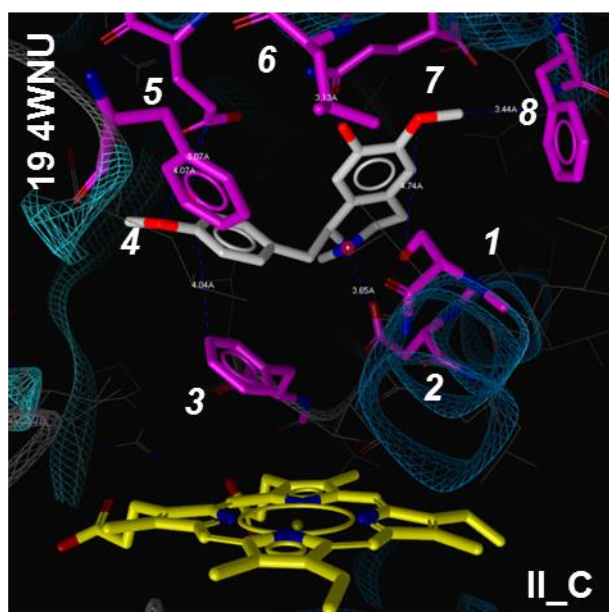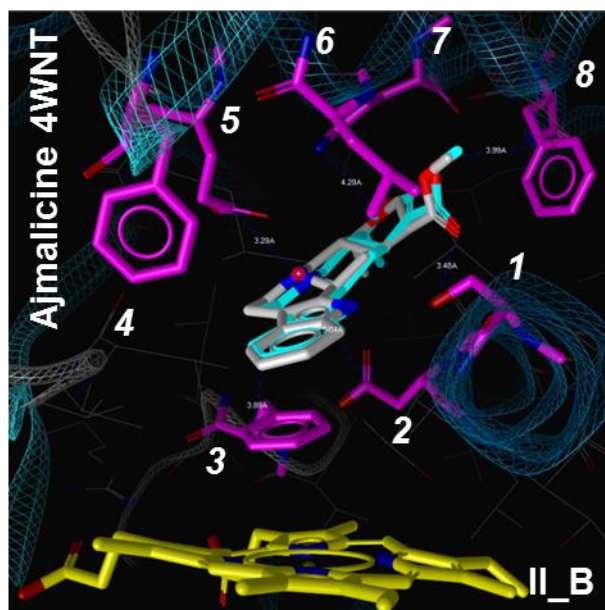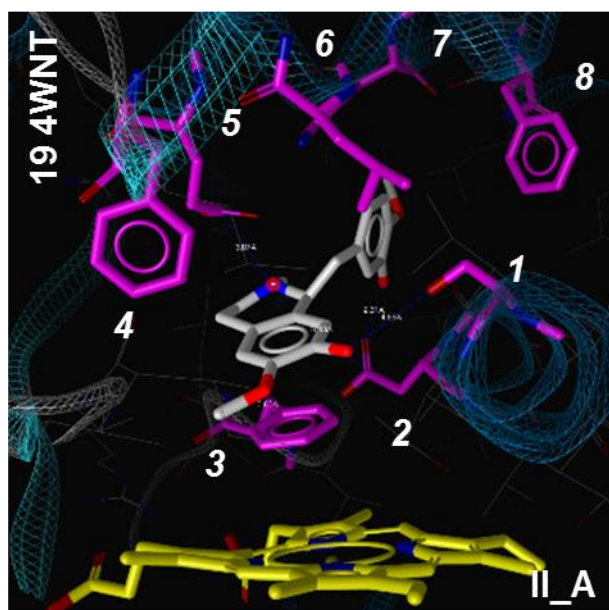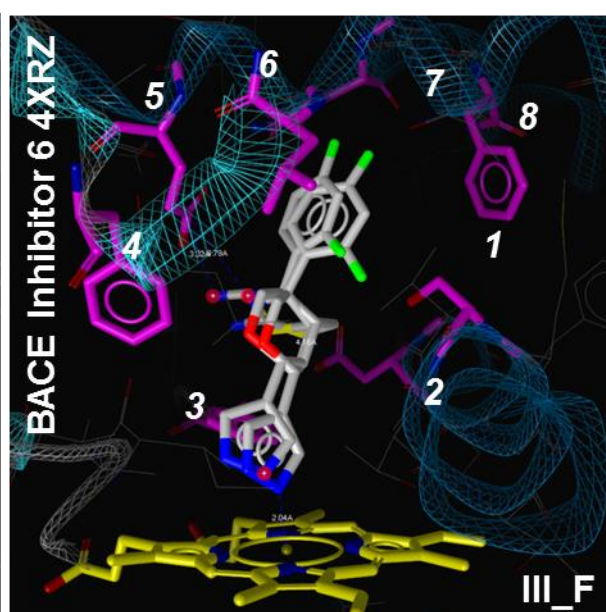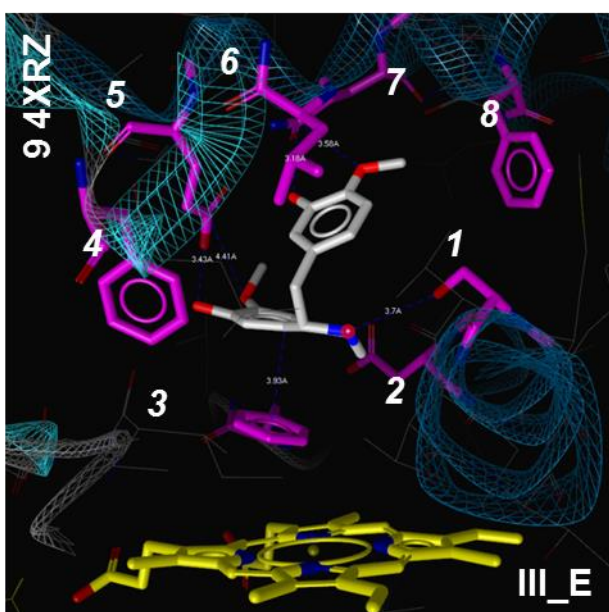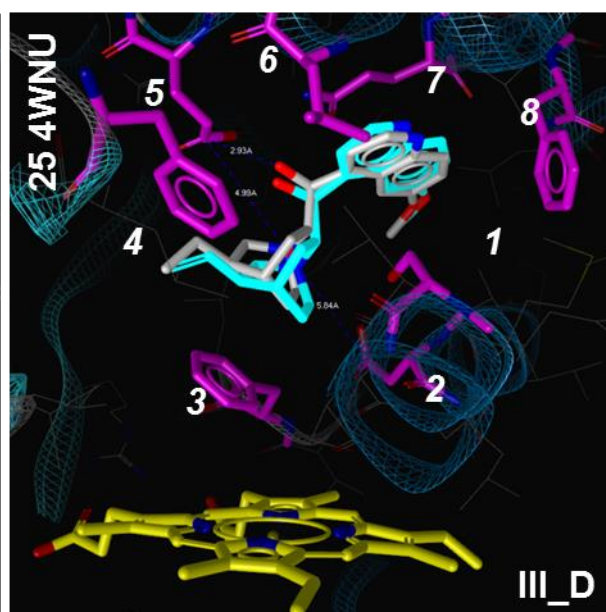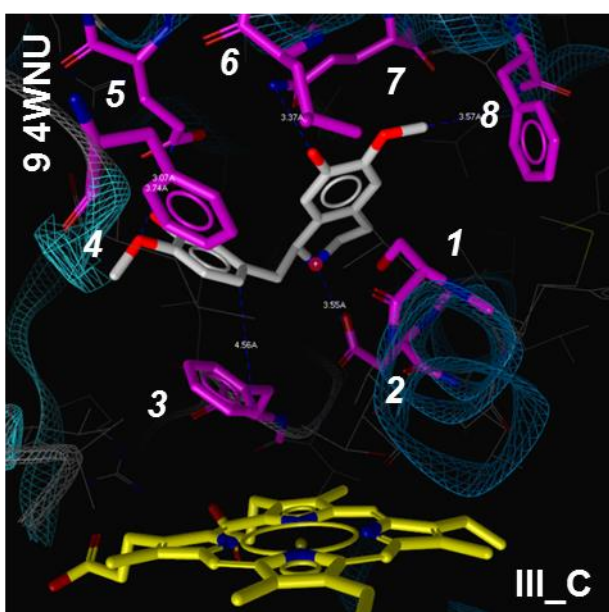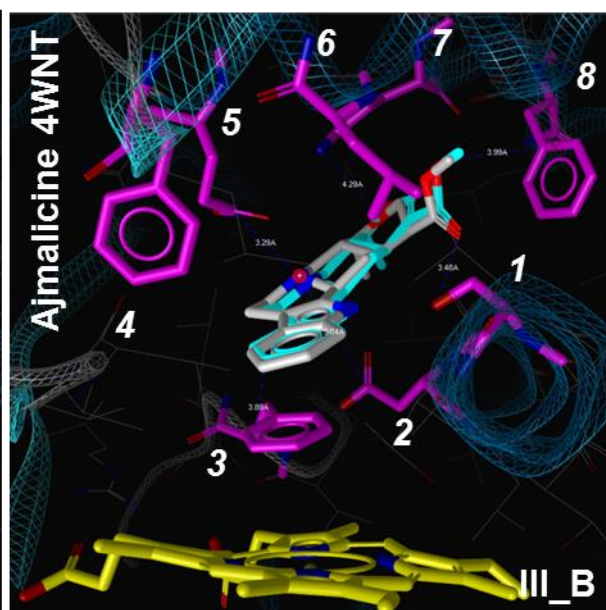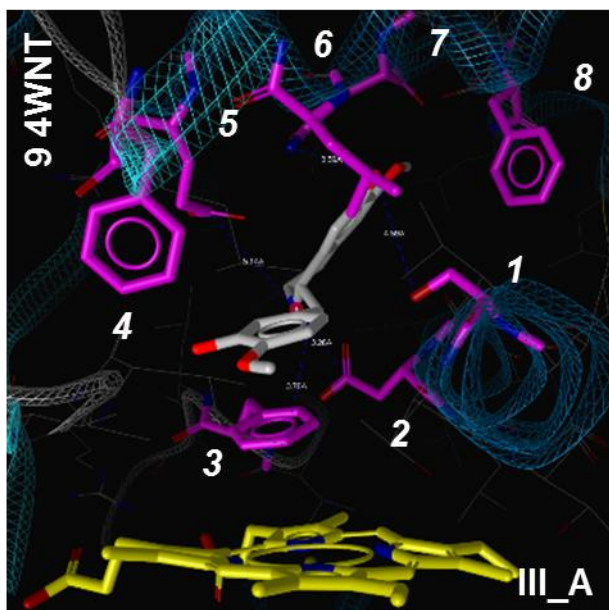
Supplementary Table S7. Compound 21 was docked in three different PDB entries. The inhibitor-enzyme interactions are listed and consensus interactions are highlighted in bold.

ligand	enzyme-AA	mode of interaction	iistance Å
21 docked in 4WNT			
ligand	enzyme-AA	mode of interaction	iistance Å
benzene ring	**Phe120**	vdW	3.1
protonated N	**Glu216**	ionic	3.6
	Gln244	electrostatic	3.8
	Ser304	H-bond	4.4
phenantridin-6-ol	Glu216	H-bond	2.8
dioxolo	**Asp301**	H-bond	4.5

ligand	enzyme-AA	mode of interaction	distance Å
21 docked in 4WNU			
ligand	enzyme-AA	mode of interaction	distance Å
benzene ring	**Phe120**	vdW	3.2
protonated N	**Glu216**	ionic	4.6
	Ser304	H-bond	3.8
phenantridin-6-ol	Ser304	H-bond	2.9
	Asp301	H-bond	3.3
dioxolo	Gln244	H-bond	4.7

ligand	enzyme-AA	mode of interaction	distance Å
21 docked in 4XRZ			
ligand	enzyme-AA	mode of interaction	distance Å
benzene ring	**Phe120**	vdW	3.6
protonated N	**Asp301**	ionic	4.1
phenantridin-6-ol	**Glu216**	H-bond	3.0

Supplementary Table S8. Compound 19 was docked in three different PDB structures. The inhibitor-enzyme interactions are listed below and the consensus interactions are highlighted in bold.

ligand	enzyme-AA	mode of interaction	distance Å
4WNT			
ligand	enzyme-AA	mode of interaction	distance Å
benzene ring (isoquinoline)	**Phe120**	vdW	3.6
protonated N	**Glu216**	ionic	3.1
hydroxyphenyl-OH	Asp301	H-bond	2.3
isoquinoline-7-OH	**Ser304**	H-bond	4.7

ligand	enzyme-AA	mode of interaction	distance Å
4WNU			
ligand	enzyme-AA	mode of interaction	distance Å
benzene ring	**Phe120**	vdW	4.0
methoxyphenyl-O	**Glu216**	H-bond	4.1
hydroxyphenyl-OH	**Glu216**	H-bond	3.1
protonated N	Asp301	ionic	3.7
isoquinoline-7-OH	Gln244	H-bond	3.1
isoquinoline-6-methoxy (O)	**Ser304**	H-bond	4.7
isoquinoline-6-methoxy (CH3)	Phe247	vdW	3.4

ligand	enzyme-AA	mode of interaction	dDistance Å
4XRZ			
ligand	enzyme-AA	mode of interaction	dDistance Å
benzene ring	**Phe120**	vdW	4.0
hydroxyphenyl-OH	Gln244	H-bond	2.8
protonated N	**Ser304**	H-bond	4.6
isoquinoline-7-OH	**Glu216**	H-bond	3.5

Supplementary Table S9. Compound 9 was docked in three different PDB structures. The inhibitor-enzyme interactions are listed below and the consensus interactions are highlighted in bold.

		4WNT	
ligand	**enzyme-AA**	**mode of interaction**	**distance Å**
benzene ring	**Phe120**	vdW	3.8
protonated N	**Glu216**	ionic	5.1
	Asp301	ionic	3.3
isoquinoline-7-OH	**Gln244**	H-bond	3.6
	Ser304	H-bond	4.6

		4WNU	
ligand	**enzyme-AA**	**mode of interaction**	**distance Å**
benzene ring	**Phe120**	vdW	4.6
methoxyphenyl-O	**Glu216**	H-bond	3.7
hydroxyphenyl-OH	**Glu216**	H-bond	3.1
protonated N	Asp301	ionic	3.6
isoquinoline-7-OH	**Gln244**	H-bond	3.4
isoquinoline-6-methoxy (CH3)	Phe247	vdW	3.6

		4XRZ	
ligand	**enzyme-AA**	**mode of interaction**	**distance Å**
benzene ring	**Phe120**	vdW	3.9
methoxyphenyl-O	**Gln244**	H-bond	3.6
hydroxyphenyl-OH	**Gln244**	H-bond	3.2
protonated N	Ser304	H-bond	3.7
isoquinoline-7-OH	**Glu216**	H-bond	3.4
isoquinoline-6-methoxy (O)	**Glu216**	H-bond	4.4

CypRules performance comparison

The direct comparison of the pharmacophore model performance with CypRules is actually rather challenging. The data set used for comparison needs to be unknown prior to both of the classifiers, because literature datasets , e.g. PubChem, will certainly contain inhibitors that have been used for training the models and thus are already known. The only data set for which this novelty was granted was our own test compound set from this study.

Both the active and the inactive compounds (Table 2 in the main manuscript) were tested on the freely accessible CypRules platform, which is a rule-based P450 inhibition prediction server (http://cyprules.cmdm.tw)[21]. For the calculations, those compounds were classified as active, which exhibited CYP2D6 IC_{50} values up to 10 µM, whereas inactives showed less than 50 % total luminescence at a concentration of 100 µM. The rule-based CYP2D6 inhibition prediction server correctly identified eight out of the thirteen actives as inhibitors. In the *in vitro* screening, the misclassified five actives *i.e.* **15**, **7**, **18**, **8** and **6** exhibited IC_{50} values of 197.8, 582.2, 2109, 4601 and 7022 nM, respectively. Looking at the six compounds that did not show CYP2D6 inhibition *in vitro*, the CypRules platform correctly identified five as inactives *i.e* **4**, **12**, **13**, **16** and **2**. Compound **10** was found to be an inhibitor, although being inactive in the *in vitro* pre-screen assay (Supplementary Table S10). In summary, CypRules correctly classified 62 % of the active and 83 % of the inactive compounds tested in this study.

Supplementary Table S10. The active compounds were tested on the freely accessible CypRules platform in order to predict their CYP2D6 inhibition.

IC_{50s} [nM]	cCompounds	CypRules
22.45	**21**	inhibitor
54.70	**19**	inhibitor
63.64	**9**	inhibitor
116.9	**14**	inhibitor
197.8	**15**	no inhibitor
380.1	**11**	inhibitor
418.6	**22**	inhibitor
582.2	**7**	no inhibitor
2109	**18**	no inhibitor
4601	**8**	no inhibitor
7022	**6**	no inhibitor
8157	**17**	inhibitor
8885	**3**	inhibitor
inactives	**4**	non inhbibitor
inactives	**10**	inhibitor
inactives	**12**	non inhbibitor
inactives	**13**	non inhbibitor
inactives	**16**	non inhbibitor
inactives	**23**	non inhbibitor

A direct comparison of the performance with the approach presented in this manuscript is difficult because only one of the compounds that was predicted as inactive by the model (compound **24**) was part of our test-set. Thus an assessment of the prospective model performance regarding compounds that are predicted to be inactive is not possible. However, the screening of the PubChem BioAssay database showed that our model successfully classified 96 % of the inactive compounds correctly.

References

1   Schuster, D., Laggner, C., Steindl, T. M. & Langer, T. Development and validation of an in silico P450 profiler based on pharmacophore models. *Current drug discovery technologies* **3**, 1-48 (2006).

2   Usia, T., Watabe, T., Kadota, S. & Tezuka, Y. Cytochrome P450 2D6 (CYP2D6) inhibitory constituents of Catharanthus roseus. *Biological & pharmaceutical bulletin* **28**, 1021-1024 (2005).

3   Li, J. *et al.* In vitro metabolic interactions between black cohosh (Cimicifuga racemosa) and tamoxifen via inhibition of cytochromes P450 2D6 and 3A4. *Xenobiotica; the fate of foreign compounds in biological systems* **12**, 1021-1030 (2011).

4   VandenBrink, B. M., Foti, R. S., Rock, D. A., Wienkers, L. C. & Wahlstrom, J. L. Prediction of CYP2D6 drug interactions from in vitro data: evidence for substrate-dependent inhibition. *Drug metabolism and disposition: the biological fate of chemicals* **40**, 47-53 (2012).

5   Zhao, Y., Hellum, B. H., Liang, A. & Nilsen, O. G. The in vitro inhibition of human CYP1A2, CYP2D6 and CYP3A4 by tetrahydropalmatine, neferine and berberine. *Phytotherapy research : PTR* **26**, 277-283 (2012).

6   Salminen, K. A. *et al.* Inhibition of human drug metabolizing cytochrome P450 enzymes by plant isoquinoline alkaloids. *Phytomedicine* **18**, 533-538 (2011).

7   Hayhurst, G. P. *et al.* Influence of phenylalanine-481 substitutions on the catalytic activity of cytochrome P450 2D6. *The Biochemical journal* **355**, 373-379 (2001).

8   Ji, H. Y. *et al.* Corydaline inhibits multiple cytochrome P450 and UDP-glucuronosyltransferase enzyme activities in human liver microsomes. *Molecules (Basel, Switzerland)* **16**, 6591-6602 (2011).

9   Vrba, J. *et al.* Metabolism of palmatine by human hepatocytes and recombinant cytochromes P450. *Journal of pharmaceutical and biomedical analysis* **102**, 193-198 (2015).

10   Han, Y. L. *et al.* In vitro inhibition of Huanglian [Rhizoma coptidis (L.)] and its six active alkaloids on six cytochrome P450 isoforms in human liver microsomes. *Phytotherapy research : PTR* **25**, 1660-1665 (2011).

11   Yao, Y. M. *et al.* Effect of sinomenine on human cytochrome P450 activity. *Clinica chimica acta; international journal of clinical chemistry* **379**, 113-118 (2007).

12   Mukkavilli, R. *et al.* Noscapine recirculates enterohepatically and induces self-clearance. *European journal of pharmaceutical sciences : official journal of the European Federation for Pharmaceutical Sciences* **77**, 90-99 (2015).

13   Ingelman-Sundberg, M. Genetic polymorphisms of cytochrome P450 2D6 (CYP2D6): clinical consequences, evolutionary aspects and functional diversity. *The pharmacogenomics journal* **5**, 6-13 (2005).

14   Sturm, S., Seger, C. & Stuppner, H. Analysis of Central European Corydalis species by nonaqueous capillary electrophoresis-electrospray ion trap mass spectrometry. *Journal of chromatography. A* **1159**, 42-50 (2007).

15   Choomuenwai, V. *et al.* The discovery, synthesis and antimalarial evaluation of natural product-based polyamine alkaloids. *Tetrahedron Letters* **54**, 5188-5191 (2013).

16   Khokhar, S. *et al.* Isolation, structure determination and cytotoxicity studies of tryptophan alkaloids from an Australian marine sponge Hyrtios sp. *Bioorganic & Medicinal Chemistry Letters* **24**, 3329-3332 (2014).

17   Jones, G., Willett, P., Glen, R. C., Leach, A. R. & Taylor, R. Development and validation of a genetic algorithm for flexible docking. *Journal of molecular biology* **267**, 727-748 (1997).

18   The Cambridge Crystallographic Data Center (2013). GOLD version 5.2, C., Cambridge, UK, https://www.ccdc.cam.ac.uk/ & solutions/csd-discovery/components/gold/.

19   Wang, A., Stout, C. D., Zhang, Q. & Johnson, E. F. Contributions of ionic interactions and protein dynamics to cytochrome P450 2D6 (CYP2D6) substrate and inhibitor binding. *The Journal of biological chemistry* **290**, 5092-5104 (2015).

20   Brodney, M. A. *et al.* Utilizing structures of CYP2D6 and BACE1 complexes to reduce risk of drug-drug interactions with a novel series of centrally efficacious BACE1 inhibitors. *Journal of medicinal chemistry* **58**, 3223-3252 (2015).

21   Shao, C. Y. *et al.* CypRules: a rule-based P450 inhibition prediction server. *Bioinformatics (Oxford, England)* **31**, 1869-1871 (2015).